The Evolution of Gas Content and Star Formation from z=3 to z=0

Francoise Combes[1] and the PHIBSS collaboration

[1]Observatoire de Paris, LERMA, College de France, CNRS, PSL, Sorbonne Univ. UPMC,
F-75014, Paris, France
email: `francoise.combes@obspm.fr`

Abstract. The cosmic star formation rate density first increases with time towards a pronounced peak 10 Gyrs ago (or z=1-2) and then slows down, dropping by more than a factor 10 since z=1. The processes at the origin of the star formation quenching are not yet well identified: either the gas is expelled by supernovae and AGN feedback, or prevented to inflow. Morphological transformation or environment effects are also invoked. Recent IRAM/NOEMA and ALMA results are reviewed about the molecular content of galaxies and its dynamics, as a function of redshift. Along the main sequence of massive star forming galaxies, the gas fraction was higher in the past (up to 80%), and galaxy disks were more unstable and more turbulent. The star formation efficiency increases with redshift, or equivalently the depletion time decreases, whatever the position of galaxies, either on the main sequence or above. Attempts have been made to determine the cosmic evolution of the H_2 density, but deeper ALMA observations are needed to effectively compare with models.

Keywords. Galaxies, Star formation, AGN, Interstellar medium, Molecular gas

1. Introduction

The cosmic star formation and its evolution through the Hubble time is now well established (e.g. Madau & Dickinson 2014). One of the main issue is to understand the rather fast winding down of star formation after z=2, both globally and also in individual galaxies. The suppression of star formation in galaxies appears rather sudden and therefore is called quenching; this has been revealed by their bimodal distribution, between a blue cloud of galaxies actively forming stars, and a red sequence of dead objects. The paucity of galaxies in an intermediate sequence (e.g. Baldry *et al.* 2006) means that the quenching time-scale is typically smaller than 1 Gyr. However the quenching mechanism is hard to identify. In a recent study of 56 GOODS galaxies at z=1.7, Mancini *et al.* (2015) found an equal proportion of AGN in both star forming and quenched galaxies, and their morphology, traced by the bulge to disk ratio or their Sersic index, was also comparable over a large range of specific star formation rate (SFR).

Since star formation is directly linked to the amount of molecular gas, it is primordial to determine the gas fraction as a function of redshift, and also the star formation efficiency (SFE), defined by the ratio between SFR and gas mass. In the recent years, a large variety of data have been obtained, with somewhat discrepant results, revealing either low or high SFE at high redshift. In sub-millimeter galaxies (SMG), and ultra-luminous starbursts (ULIRGs) the SFE increases with redshift, and the depletion time (the inverse of SFE) which is of the order of 0.5-1Gyr for ULIRGs at z∼ 0 becomes as low as 10-100 Myr at z=1-2 (Greve *et al.* 2005, Combes *et al.* 2011, 2013). But there exists a population of massive BzK galaxies, selected from their near-IR and optical colors, which are also actively forming stars (they are ULIRGs), but with a lower efficiency, with a depletion time-scale of the order of 0.3 Gyr at z∼ 1.5 (Daddi *et al.* 2008), i.e. similar to local

240

ULIRGs. This might be due to their extended molecular component (10 kpc scales), and their low density state, revealed by their low excitation: the CO emission as a function of the upper level J peaks at $J = 3$, as in the Milky Way (Dannerbauer *et al.*2009), justifying the adoption of the standard CO-to-H_2 conversion factor (5 times that adopted for ULIRGs). Let us recall that local main-sequence galaxies, such as the Milky Way, have a depletion time-scale of the order of 2 Gyr (Bigiel *et al.* 2011).

2. Starburst galaxies

In a recent work with IRAM and ALMA, Silverman *et al.* (2015) detected CO emission in 7 galaxies from the COSMOS survey, with SFR$\sim$ 300-800 M$_\odot$/yr, at $1.4 < z < 1.7$. Their gas fraction was determined to be $\sim$ 30-50%, and their global SFE is enhanced, although the objects are unresolved, and the starbursting regions cannot be separated.

To trace redshift evolution and in particular the winding down of star formation after z=1, the intermediate redshift epoch $0.2 < z < 1$ is a key region to explore. We have observed the gas content of ULIRGs at these intermediate z, to make the link with local starbursts (Combes *et al.* 2011, 2013). Out of 69 ULIRG, 33 were detected in CO emission, with variable excitation. Some of the objects have a lower H_2 density, which can be explained in terms of at least two components. The objects for which an interferometric map is available show the separation of the molecular emission in a nuclear starburst and an extended gas disk of scale $\sim$20 kpc. The presence of such an extended component may explain lower SFE, in particular when low gas excitation suggests a higher CO-to-H_2 conversion ratio.

This study at intermediate z, compared to all other starburst data, showed that both gas fraction and SFE increase with redshift, by a factor 3±1, between z=0 and 1, with or without taking into account upper limits.

Recently, the Bzk galaxies at z=1.5, which show globally low excitation of the CO lines at low J were observed to have quite high CO(5-4) fluxes, revealing a second component of more excited, denser and warmer molecular gas (Daddi *et al.* 2015). For this excited component, the objects have the same correlations than for ULIRGs, confirming that the starburst occurs either in a separate nuclear region, or in hot and dense star forming clumps. In local starbursts, the total CO SLEDs observed with Herschel reveal a very large variety of shapes, with several molecular components (Mashian *et al.*2015), suggesting that the overall CO-to-H_2 conversion ratio could explore even wider ranges than expected, from $\alpha =0.4$ to 5 M$_\odot$/(K km/s pc^2) for the M(H_2) to L'CO ratio.

3. Main sequence galaxies

Most of the cosmic star formation ($\sim$ 90%) occurs in the main sequence galaxies, and only about 10% in starbursts. The main sequence is clearly defined in an SFR versus stellar mass diagram as a power-law with slope slightly lower than 1. This power-law is similar at all redshift ranges, but the zero point is increasing with redshift, following the evolution of the cosmic star formation rate density described in the introduction. Large surveys of hundred thousands of galaxies locally (SDSS) or at high redshift (GOODS, COSMOS, ..) have shown a correlation between morphology and stellar populations since z$\sim$2.5 (Wuyts *et al.* 2011): blue star forming galaxies on the main sequence are exponential disks (Sersic index near 1), while quiescent red systems are of de Vaucouleurs type (Sersic index more near 4).

With the goal to explore the molecular gas content of main sequence galaxies, we undertook the PHIBSS project (Plateau de Bure HIgh z Blue Sequence Survey, Tacconi
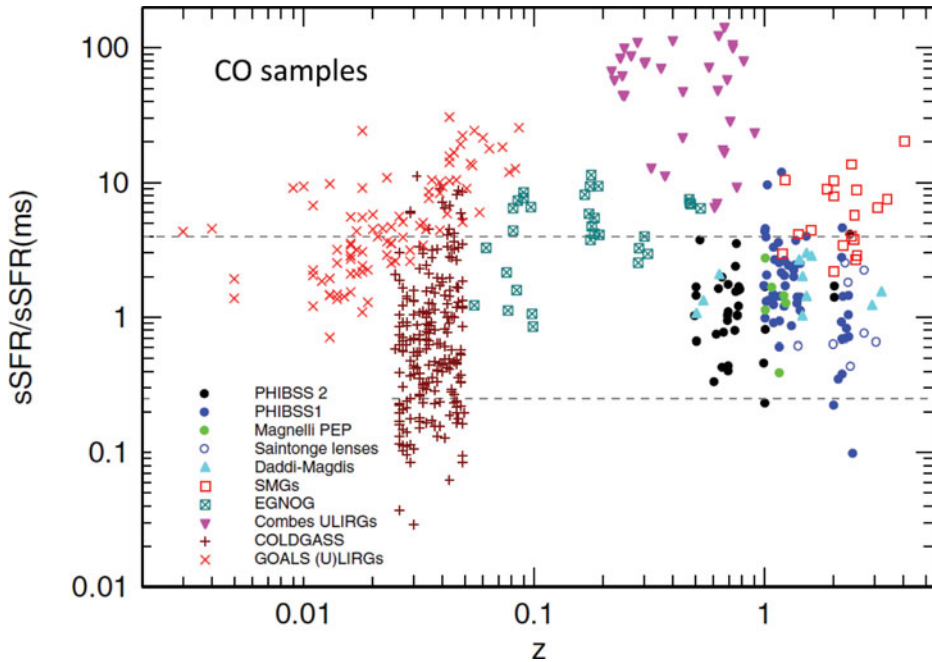
Figure 1. Distribution in the redshift versus specific star-formation rate plane of all the star forming galaxies with CO flux measurements found in the literature, compared with the PHIBSS data by Genzel *et al.* (2015). The sSFR on the vertical axis is normalized to the main sequence (ms) value of sSFR at a given mass and redshift, according to the scaling relation given by Whitaker *et al.* (2012). The membership to the main sequence is defined by the two horizontal dashed lines, situated at ± 0.6 dex from the mid MS line. *A color version is available online.*

et al. 2010, 2013). In the first part of the project, 52 galaxies were detected at IRAM in the CO(3-2) line at z=1.2 and 2.3. The targets were selected to be massive ($M_* > 2.5 \, 10^{10} \, M_\odot$) star forming galaxies (SFR > 30 $M_\odot$/yr). Adopting a standard CO-to-H_2 conversion ratio for these main sequence objects, molecular masses were found between 10^{10} and $3 \, 10^{11} \, M_\odot$, corresponding to gas fraction in average of 33% at z=1.2 and 47% at z=2.3. The SFE was found to increase slightly with z, and the depletion time scale is in average 0.7 Gyr at z=1.2.

   The CO detection rate was quite high (>85%), in these normal massive Star Forming Galaxies (SFG). Some were mapped at high spatial resolution, and a rather regular velocity field was found, confirming the absence of major mergers. At z=1.2, it was possible to resolve four galaxy disks in clumps with the help of the velocity information, both with CO and [OII] lines (gas content and SFR), since there is a good correlation between molecular and ionised gas. This allowed us to draw a resolved Kennicutt-Schmidt (KS) relation (Freundlich *et al.* 2013). The high-z points extend the local KS relation towards high gas and SFR surface densities, with the same slope. For one galaxy at z=1.5, it was possible to observe the Hα line at high resolution from the ground (Genzel *et al.* 2013). The KS slope depends strongly on the dust extinction model adopted, but falls around 1.

   The evolution of specific SFR with redshift was compatible with the results of optical surveys, provided that the depletion time is varying on the main sequence as t_{dep}=1.5/(1+z) Gyr. The PHIBSS project is now being extended with the goal of observing CO lines in about 150 galaxies, exploring also intermediate redshifts (z=0.5-0.7), and some galaxies departing from the main sequence, either starbursts above the MS or
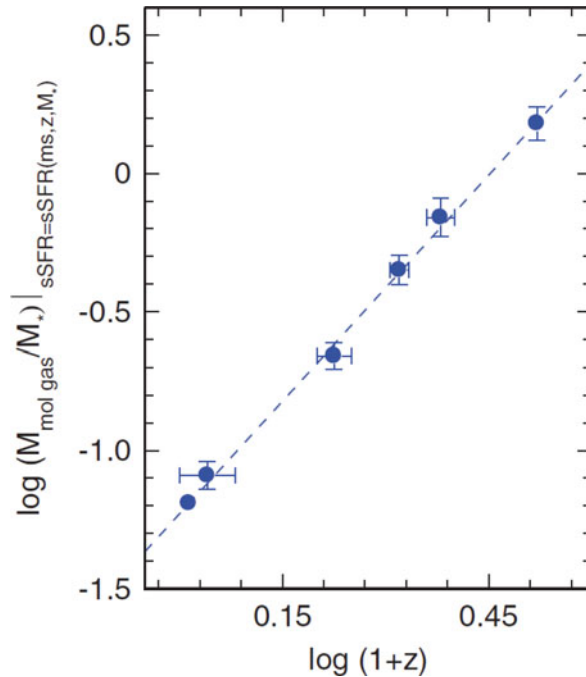
Figure 2. Ratio of the molecular to stellar mass versus redshift, for galaxies on the main-sequence (Genzel *et al.* 2015). The best linear fit has a slope of 2.71 (dashed line).

quiescent galaxies below (PHIBSS2). Detecting smaller masses, and bright galaxies with more spatial resolution and/or more molecular lines in addition will be attempted with ALMA.

The first results and the scaling relations obtained on the main sequence, by comparison with all other data with CO detections at high redshift (cf Fig 1), were presented in Genzel *et al.* (2015). On the MS, the gas fraction increases regularly with z, as shown in Fig 2.

Fig 3 displays the depletion time as a function of redshift, for the galaxies on the main sequence. There is a slight decrease, and the effect depends on the way the molecular gas content is estimated, either from the CO line, or from the dust emission.

A recent survey with ALMA of the continuum dust emission of 180 star forming galaxies between z=1 and 6.4 results in slightly different results (Scoville *et al.* 2015). The gas fraction estimated from the dust emission, assuming a constant dust temperature, is also highly increasing with redshift, reaching values as high as 50-80%. The depletion time-scale is found to be the same for starbursts and main sequence galaxies; it decreases strongly with redshift, to reach 200 Myr at z> 1, therefore 10 times lower than for local MS galaxies.

4. The cosmic H_2 density

One of the key issues to understand the cosmic star formation history is to observe the cosmic evolution of the H_2 density. Theoretical considerations and semi-analytical models predict that the molecular gas density must increase with redshift, and dominate over the atomic gas in galaxies (Obreschkow & Rawlings, 2009, Obreschkow *et al.* 2009). The phase transition from atomic to molecular hydrogen is favored by pressure (Blitz & Rosolowsky 2006), while surface density and consequently the pressure is higher in high-z
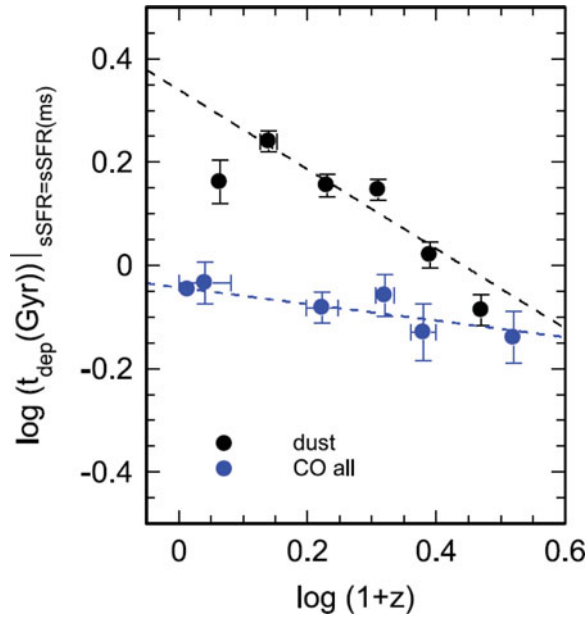
Figure 3. Depletion time versus redshift for galaxies on the main sequence, computed from the dust emission (black circles), and from the CO lines (blue circles). The best linear fit has a slope of –0.77 (black dashed line). *A color version is available online.*

galaxies. Models predict a molecular-to-atomic ratio H_2/HI varying as $(1+z)^m$, with m as high as 1.6. Some models however predict flatter evolutions of the H_2 density at high z (Lagos *et al.* 2011, Popping *et al.* 2014).

Decarli *et al.* (2014) and Walter *et al.* (2014) have attempted to constrain the H_2 density by observing a large cosmic volume of $\sim$7000 Mpc^3, in the Hubble deep field North with Plateau de Bure. They separate the results in three redshift bins: z<0.45, 1.01<z<1.89 and z>2. A blind molecular line survey has been carried out through scanning the whole 3mm band. The blind detection of 17 CO lines, together with the upper limits obtained by stacking the observations towards spectroscopically identified objects, constrain the CO luminosity functions at the corresponding redshifts. The results show that optical/mid-IR bright galaxies contribute less than 50% to the star formation rate density at $1 < z < 3$, and the normalised density $\Omega(H_2)$ at high z tends to be higher than the predictions.

It might be easier and certainly quicker to determine the evolution of the H_2 density from dust emission surveys. A recent 870μm continuum survey with ALMA of 99 SMG in the Extended Chandra Deep Field South (Swinbank *et al.* 2014) has discovered that the well detected sources ($S_{870} > 4.2$ mJy) are in average ULIRGs with SFR=300 $M_\odot$/yr, and dust temperatures of 32 K. They contribute to only 1-2% of SFR. The extrapolation of the counts down to $S_{870} > 1$ mJy through stacking shows that these sources contribute to 20% of the cosmic star formation density over z=1-4 (see Fig 4). Deriving H_2 masses from dust masses, the average SFE is found rather high, with depletion time-scale of 130 Myr.
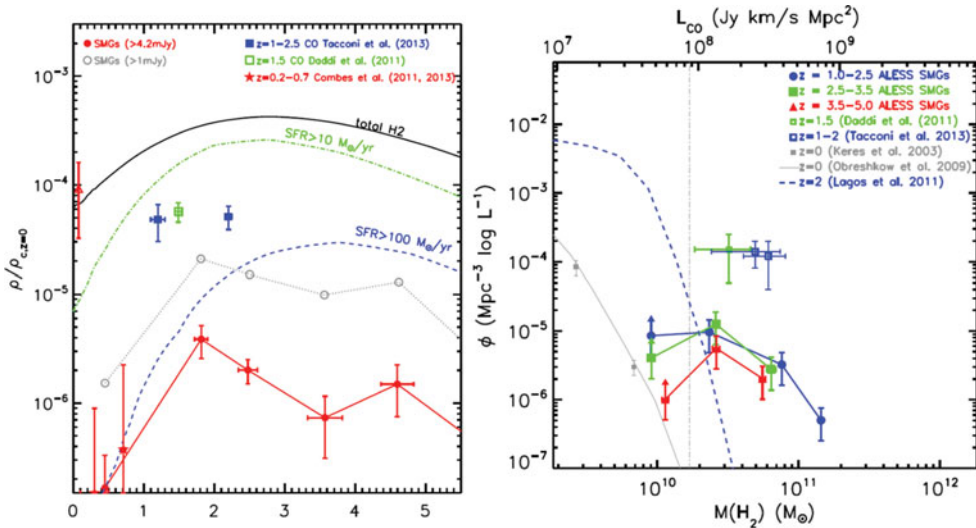
Figure 4. Left: The normalised H_2 density $\Omega(H_2)$ as a function of redshift, for SMG and other high-z starbursts (Swinbank *et al.*2014, Combes *et al.* 2013) in red, compared to main sequence galaxies in blue (Tacconi *et al.*2013). The dashed lines are the model predictions, for different SFR (Lagos *et al.*2011). **Right:** The H_2 mass function for SMG and main sequence galaxies compared with models. The main sequence galaxies at z=1.5 (green) are from Daddi *et al.* (2010) and at z=1-2 (blue) from Tacconi *et al.* (2013). They are well above the predictions at z=2 by Lagos *et al.*(2011) indicated by the blue dashed curve. From Swinbank *et al.* (2014). *A color version is available online.*

5. Conclusions

It is now well established that galaxies at high redshift have a larger gas fraction than local ones, whatever their position on the main sequence or above, in the starburst domain. The gas fraction can reach 50% and above.

There is not yet a consensus on the exact evolution of the star formation efficiency with redshift. The inverse of the SFE, the depletion time scale, is decreasing with redshift, however the amplitude of its variation with z is still debated. The various results depend on the way to estimate the total molecular gas amount, either from CO lines or from dust emission. The results may also depend on the definition of the Main Sequence (e.g. Renzini & Peng, 2015).

A higher SFE at high z might be explained by a higher surface density of molecular gas, if the Kennicutt-Schmidt relation is non-linear, which is not yet well known. Alternatively, a starburst can be triggered in nuclear regions when the gas is concentrated. Diagnostics could be searched for with CO excitation and the observation of several J lines, and also dense gas tracers (HCN, HCO^+).

ALMA observations begin to estimate the evolution of the molecular gas mass in galaxies, however we are still far from a total census of $\Omega(H_2)$ as a function of redshift.

References

Baldry, I. K., Balogh, M. L., Bower, R. G. *et al.* 2006, *MNRAS* 373, 469
Bigiel, F., Leroy, A. K., Walter, F. *et al.* 2011, *ApJ*, 730, L13
Blitz L., Rosolowsky E. 2006, *ApJ*, 650, 933
Combes, F., Garcia-Burillo, S., Braine, J. *et al.* 2011 *A&A* 528, A124
Combes, F., Garcia-Burillo, S., Braine, J. *et al.* 2013 *A&A* 550, A41

Daddi, E., Dannerbauer, H., Elbaz, D. *et al.* 2008, *ApJ*, 673, L21

Daddi, E., Bournaud, F., Walter, F. *et al.* 2010, *ApJ*, 713, 686

Daddi, E., Dannerbauer, H., Liu, D. *et al.* 2015, *A&A* 577, A46

Dannerbauer, H., Daddi, E., Riechers, D. A. *et al.* 2009, *ApJ*, 698, L178

Decarli, R., Walter, F., Carilli, C. *et al.* 2014, *ApJ*, 782, 78

Freundlich, J., Combes, F., Tacconi, L. J. *et al.* 2013, *A&A* 553, A130

Genzel, R., Tacconi, L. J., Kurk, J. *et al.* 2013, *ApJ*, 773, 68

Genzel, R., Tacconi, L. J., Lutz, D. *et al.* 2015, *ApJ*, 800, 20

Greve, T. R., Bertoldi, F., Smail, I. *et al.* 2005 *MNRAS* 359, 1165

Lagos C. d P., Baugh C. M., Lacey C. G. *et al.* 2011, *MNRAS* 418, 1649

Madau, P. & Dickinson, M. 2014, *ARAA* 52, 415

Mancini, C., Renzini, A., Daddi, E. *et al.* 2015, *MNRAS* 450, 763

Mashian, N., Sturm, E., Sternberg, A. *et al.* 2015, *ApJ*, 802, 81

Obreschkow D., Croton D., de Lucia G. *et al.* 2009, *ApJ*, 698, 1467

Obreschkow D., Rawlings S.: 2009, *ApJ*, 696, L129

Popping G., Somerville R. S., Trager S. C., 2014, *MNRAS*, 442, 2398

Renzini, A. & Peng, Y.-J. 2015, *ApJ*, 801, L29

Scoville, N., Sheth, K., Aussel, H. *et al.* 2015, *ApJ*, in press, arXiv1505-02159

Silverman, J. D., Daddi, E., Rodighiero, G. *et al.* 2015, *ApJ*, in press, arXiv1505-04977

Swinbank A. M., Simpson J. M., Smail I., *et al.* 2014, *MNRAS*, 438, 1267

Tacconi, L. J., Genzel, R., Neri, R. *et al.* 2010, *Nature*, 463, 781

Tacconi, L. J., Neri, R., Genzel, R. *et al.* 2013, *ApJ*, 768, 74

Walter, F., Decarli, R., Sargent, M. *et al.* 2014, *ApJ*, 782, 79

Whitaker, K. E., van Dokkum, P. G., Brammer, G., & Franx, M. 2012, *ApJ*, 754, L29

Wuyts, S., Förster Schreiber, N. M., van der Wel, A. *et al.* 2011 *ApJ*, 742, 96